Molecular Basis of the Receptor Interactions of Polysialic Acid (polySia), polySia Mimetics, and Sulfated Polysaccharides

Article *in* ChemMedChem · May 2016

DOI: 10.1002/cmdc.201500609

CITATIONS
12

READS
440

19 authors, including:

Gabriele Loers
University of Hamburg
96 PUBLICATIONS **2,192** CITATIONS

SEE PROFILE

Rolf Boelens
Utrecht University
421 PUBLICATIONS **21,015** CITATIONS

SEE PROFILE

Stefan Kraan
The Seaweed Company
40 PUBLICATIONS **2,373** CITATIONS

SEE PROFILE

ChemPubSoc Europe

DOI: 10.1002/cmdc.201500609

CHEMMEDCHEM Full Papers

Molecular Basis of the Receptor Interactions of Polysialic Acid (polySia), polySia Mimetics, and Sulfated Polysaccharides

Ruiyan Zhang,[a, b] Gabriele Loers,[c] Melitta Schachner,[c, d] Rolf Boelens,[e] Hans Wienk,[e] Simone Siebert,[a] Thomas Eckert,[f, g] Stefan Kraan,[h] Miguel A. Rojas-Macias,[f] Thomas Lütteke,[f] Sebastian P. Galuska,[i] Axel Scheidig,[b] Athanasios K. Petridis,[j] Songping Liang,[k] Martin Billeter,[l] Roland Schauer,[m] Jürgen Steinmeyer,[n] Jens-Michael Schröder,[o] and Hans-Christian Siebert*[a]

Polysialic acid (polySia) and polySia glycomimetic molecules support nerve cell regeneration, differentiation, and neuronal plasticity. With a combination of biophysical and biochemical methods, as well as data mining and molecular modeling techniques, it is possible to correlate specific ligand–receptor interactions with biochemical processes and in vivo studies that focus on the potential therapeutic impact of polySia, polySia glycomimetics, and sulfated polysaccharides in neuronal diseases. With this strategy, the receptor interactions of polySia and polySia mimetics can be understood on a submolecular level. As the HNK-1 glycan also enhances neuronal functions, we tested whether similar sulfated oligo- and polysaccharides from seaweed could be suitable, in addition to polySia, for finding potential new routes into patient care focusing on an improved cure for various neuronal diseases. The knowledge obtained here on the structural interplay between polySia or sulfated polysaccharides and their receptors can be exploited to develop new drugs and application routes for the treatment of neurological diseases and dysfunctions.

Introduction

A deeper insight into the biological role of polysialic acid (polySia) and sulfated polysaccharides is possible when we understand more details about the complementarity of structure and function on a submolecular level by combining cell biological, biochemical, and biophysical methods. The correlations between neuro-oncological mechanisms and nerve cell regen-

[a] R. Zhang, S. Siebert, Prof. Dr. H.-C. Siebert
RI-B-NT: Research Institute of Bioinformatics and Nanotechnology, Franziusallee 177, 24148 Kiel (Germany)
E-mail: hcsiebert@aol.com

[b] R. Zhang, Prof. Dr. A. Scheidig
Zoological Institute, Department of Structural Biology, Kiel University, Am Botanischen Garten 1–9, 24118 Kiel (Germany)

[c] Dr. G. Loers, Prof. Dr. M. Schachner
Center for Molecular Neurobiology Hamburg, University Medical Center Hamburg-Eppendorf, University of Hamburg, Falkenried 94, 20251 Hamburg (Germany)

[d] Prof. Dr. M. Schachner
Center for Neuroscience, Shantou University Medical College, 22 Xin Ling Road, Shantou, Guangdong 515041 (China)

[e] Prof. Dr. R. Boelens, Dr. H. Wienk
Bijvoet Center for Biomolecular Research, NMR Spectroscopy, Utrecht University, Padualaan 8, 3584 CH Utrecht (The Netherlands)

[f] Dr. T. Eckert, M. A. Rojas-Macias, Dr. T. Lütteke
Institute of Veterinary Physiology and Biochemistry, Fachbereich Veterinärmedizin, Justus-Liebig-Universität Gießen, Frankfurter Str. 100, 35392 Gießen (Germany)

[g] Dr. T. Eckert
Clinic for Obstetrics, Gynecology and Andrology of Large and Small Animals, Justus-Liebig-Universität Gießen, Frankfurter Str. 106, 35392 Gießen (Germany)

[h] Dr. S. Kraan
Ocean Harvest Technology Ltd., N17 Business Park, Milltown, County Galway, (Ireland)

[i] Dr. S. P. Galuska
Institute of Biochemistry, Faculty of Medicine, Justus-Liebig-Universität Gießen Friedrichstr. 24, 35392 Gießen (Germany)

[j] Dr. A. K. Petridis
Department of Neurosurgery, Klinikum Duisburg GmbH, Zu den Rehwiesen 9, 47055 Duisburg (Germany)

[k] Prof. Dr. S. Liang
College of Life Sciences, Hunan Normal University, 410081 Changsha (China)

[l] Prof. Dr. M. Billeter
Department of Chemistry and Molecular Biology, University of Gothenburg, Box 100, 40530 Gothenburg (Sweden)

[m] Prof. Dr. R. Schauer
Institute of Biochemistry, Kiel University, Olshausenstr. 40, 24098 Kiel (Germany)

[n] Prof. Dr. J. Steinmeyer
Orthopaedic Research Laboratories, Department of Orthopaedic Surgery, University Hospital Giessen and Marburg GmbH, Paul-Meimberg-Str. 3, 35392 Gießen (Germany)

[o] Prof. Dr. J.-M. Schröder
Department of Dermatology, University Hospital Schleswig-Holstein, Campus Kiel, 24105 Kiel (Germany)

Supporting information for this article can be found under http://dx.doi.org/10.1002/cmdc.201500609.

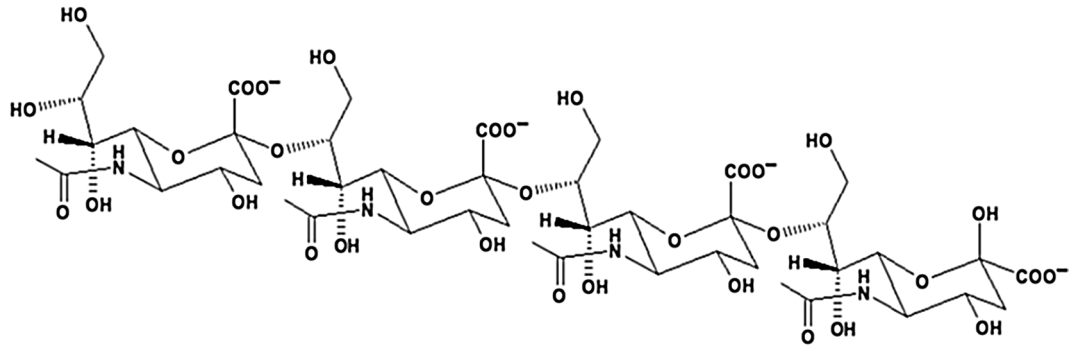

Figure 1. Illustration of a sialic acid tetramer consisting of four α2,8-linked Neu5Ac residues.

eration processes on a nanoscale size need to be determined for glycans, because sialic acids, and especially the α2,8-linked polysialic acid molecules (Figure 1), are involved in diverse cell differentiation processes depending on the organ, cell type, and stage of maturation.[1–7] When the impact of certain glycan epitopes on these processes is analyzed with the aim of improving therapeutic strategies, it is essential to describe the glycan–receptor interactions at atomic resolution. Therefore, it is important to determine the crucial functional groups on the ligand and on the receptor side, as well as the positions of these functional groups in relation to each other. As drug analysis and drug design are our goals, we looked for common principles that are characteristic of these ligand–receptor interactions. For example, in the respiratory and reproductive systems, polySia attached to neural cell adhesion molecule (NCAM) is believed to counteract the cytotoxic characteristics of extracellular histones, which are generated during inflammation.[8,9a] In contrast, in the neuronal system, the interaction of polySia with histone H1 seems to be important for regeneration phenomena.[10] Histone H1 directly binds to polySia in the extracellular space and at the plasma membrane, as shown for cultured cerebellar neurons. Immunostaining of live cerebellar neurons and Schwann cells confirmed that an extracellular pool of histone H1 co-localizes with polySia at the cell surface and stimulates neuritogenesis and process formation as well as proliferation of Schwann cells in vitro. Furthermore, migration of neural precursor cells by a polySia-dependent mechanism also indicates that histone H1 is active extracellularly. These in vitro observations suggest an important functional role for the interaction between histone H1 and polySia, not only for nervous system development, but also for regeneration in adults. Indeed, histone H1 improved functional recovery, axon regrowth, and precision of reinnervation of the motor branch in adult mice with femoral nerve injury.[10] In contrast to histone H1, the myristoylated alanine-rich C kinase substrate (MARCKS) does not interact with polySia extracellularly but within the plasma membrane.[11] We especially focused on the polySia receptor MARCKS in this study in order to find out whether this receptor binds polySia glycomimetic molecules in a similar way as it does polySia fragments. The highly basic effector domain of MARCKS (MARCKS-ED) that we analyzed here interacts with polySia at the cell membrane and mediates the membrane insertion of MARCKS.

In addition to the family of negatively charged sialic acids and their polymers or mimicking molecules, sulfated carbohydrates like the HNK-1 epitope play important roles as contact points on neuronal cells. In addition, the HNK-1 carbohydrate regulates migration of neural crest cells, synaptic plasticity, learning and memory, and preferential motor reinnervation.[12] When sulfated carbohydrates from marine organisms (e.g., algae) that express many different sulfated glycans can be identified which act in a similar manner to the HNK-1 glycan, this may identify an important source from which such bioactive molecules can be obtained. These sulfated polysaccharides can be used for the development of novel therapeutic drugs complementary to those generated on the basis of polySia and polySia mimicking molecules. Only the strategic combination of biochemical and biophysical methods allows a clear interpretation of how glycans influence and regulate the corresponding biochemical processes in different biological systems. Surface plasmon resonance (SPR) techniques, for instance, estimate how strongly carbohydrate self-recognition, which mediates marine sponge cellular adhesion, depends on the occurrence of sulfate groups on the carbohydrate residues.[13] Other biophysical devices, like quartz crystal microbalances (QCMs) or microarrays, are helpful tools to correlate physical–chemical parameters with neurobiological functions.[14,15] Here, a combination of NMR, molecular modeling (including docking algorithms and quantum chemical calculations), and data mining tools was identified as a suitable strategy to examine the interaction of polySia and sulfated carbohydrates with their cognate receptors on a submolecular level. Due to their important role in nervous system regeneration and neuro-oncological processes, polySia receptors (e.g., lectins) are of the highest clinical importance.[16–19] The involvement of polySia and sulfated oligosaccharides, such as the HNK-1 epitope, in neurite outgrowth allows development of new therapeutic strategies with strong supportive impact on nervous system regeneration in mammals.[7,20–24] NCAM, as well as other polySia-carrying proteins, which are neuropilin-2 and the synaptic cell adhesion molecule SynCAM1, interact with these receptors through a repeating unit, the disaccharide α2,8-linked sialic acid building block. In our study, we focused on the polySia receptors MARCKS, α-defensins HNP 1, 2, 3 and HD5, and a lectin from the Chinese bird-hunting spider, SHL-1, to describe the molecular basis of polySia–protein interactions. In combination with

our data on sulfated polysaccharides, we were able to define the functional groups that are responsible for the specific interactions between polySia receptors and their ligands. The *N*-acetyl and carboxyl groups of the Neu5Ac residue are of importance for ligand recognition, similar to the way in which the sulfate groups from algae polysaccharides or the HNK-1 glycan determine their biological function. As the α2,8 linkage between two Neu5Ac residues defines the minimum building unit of polySia, we also have to consider the conformational dynamics of these linkages. As we can learn from the ligand–receptor interactions in which polySia glycomimetics are involved, the shape of the molecule is not the only property that is responsible for initiating a specific binding process. Dynamic aspects that are correlated to the structural flexibility or rigidity of the molecules under study must be considered as well.

Results and Discussion

Molecular modeling and data mining

Sialic acid receptors of different origin have structural similarities in the architecture of their carbohydrate recognition domains (CRDs), pertaining, for instance, to the three-dimensional (3D) arrangement of certain amino acid residues.[19,24–27,28] In addition to arginine residues, aromatic amino acids, such as tryptophan and tyrosine are often involved in these interactions, leading to a stable complex formation. Due to its involvement in neuronal processes, MARCKS-ED was chosen as paradigmatic polySia mini-receptor. Lysine is the most frequently occurring amino acid residue (12 times) in the sequence. However, arginine, serine, and asparagine residues, which frequently occur in the vicinity of receptor-bound sialic acids (Figure 3) are also present in the MARCKS-ED sequence (Figure 2) and must be considered as important contributors

MARCKS-ED: KKKKKRFSFKKSFKLSGFSFKKNKK
MARCKS-ED control: KKKKKR**A**S**A**KKS**A**KLSG**A**S**A**KKNKK

Figure 2. Amino acid sequence of the effector domain of the myristoylated alanine-rich kinase C substrate (MARCKS-ED, top) and the MARCKS-ED control peptide (bottom). Phenylalanines that were changed to alanines in the control peptide are highlighted in bold.

for the specific binding process.

No tryptophan or tyrosine residues exist in the MARCKS-ED sequence. The phenylalanine residues in the sequence are of special interest with respect to polySia binding specificity mediated by aromatic residues. Five phenylalanine residues in the MARCKS-ED sequence are responsible for the nonpolar aromatic interactions with the carbohydrate moieties and support the four serine and the single arginine and asparagine residues to bind polySia in a specific way. Bioinformatic tools, such as data mining approaches for a general analysis of all protein–sialic acid complexes in the RCSB Protein Data Bank (PDB), show that arginine, serine, tyrosine, and tryptophan residues are the most frequently occurring amino acid residues in

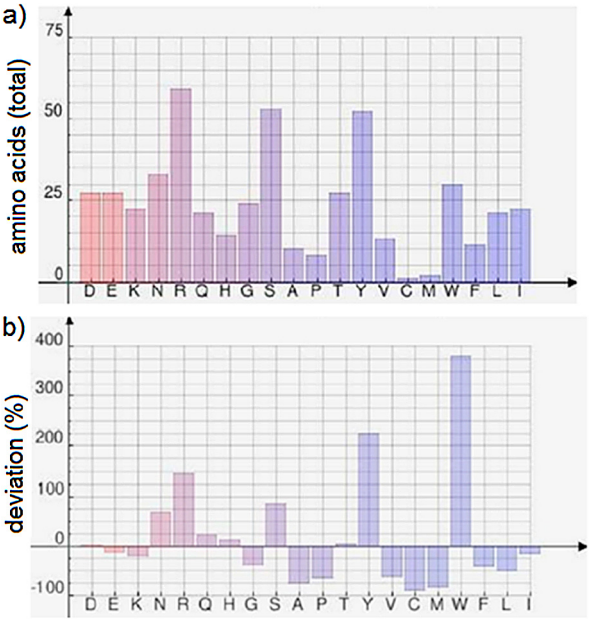

Figure 3. Data mining results with respect to sialic acid–protein complexes. Amino acid residues in the vicinity of sialic acid (basic form: Neu5Ac) according to their occurrence in the PDB (www.rcsb.org/pdb/). A dataset of glycan-binding proteins was analyzed with GlyVicinity (www.glycosciences.de/tools/glyvicinity/)[24] at a redundancy level of 70%. a) Total number of amino acids that are in the vicinity of sialic acid residues. b) Deviation (as a percentage) from the natural abundance of the corresponding amino acid residues; negative values signify that these amino acids are less frequently found in close contact with the sialic acid residues than in an average protein, whereas positive values indicate overrepresentation of amino acids in the vicinity of sialic acid residues.

the vicinity of bound sialic acids (Figure 3). Different amino acids occur in sialic acid receptors with variable abundance; therefore, their absolute values are not well suited to characterize residue binding sites (Figure 3a). Instead, the percentage deviation from their natural abundance is more appropriate for this purpose (Figure 3b). The most prominent binding partners that stabilize sialic acid–protein complexes are tryptophan, tyrosine, and arginine residues. Lysine residues are underrepresented when sialic acids are involved in binding. This means they show a negative deviation from the natural abundance, indicating that they are less frequently found in the vicinity of sialic acids than in the average of all proteins. As described in detail below, our NMR results clearly indicate that specific interactions between the lysine-rich MARCKS-ED peptide and sialic acid residues exist. Although tyrosine and tryptophan do not occur in the MARCKS-ED, arginine, asparagine, and serine are present and overrepresented in other sialic acid receptors (Figure 3b).

The picture becomes clearer when other negatively charged saccharides besides sialic acid are analyzed. Focusing on sulfate groups, the data mining approach shows that lysine is overrepresented in the vicinity of this functional group (Figure 4a). In addition to lysine residues, arginine residues are likely to primarily bind, due to their preferred vicinity to sulfate groups and uronic acid. Sulfate groups occur in different glycans, such as in the sulfated form of the HNK-1 epitope, where

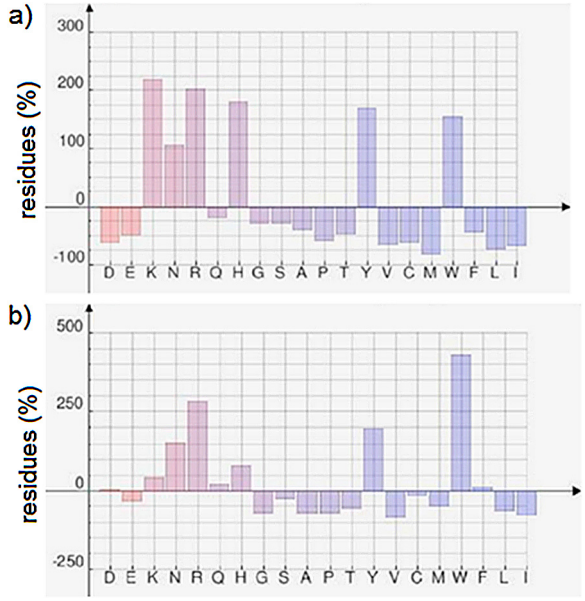

Figure 4. Data mining results with respect to carbohydrate–protein complexes in which sulfated carbohydrates and/or uronic acids occur as ligands. Amino acid residues in the vicinity of a) sulfated carbohydrates and b) uronic acids, according to their occurrence in the PDB. A dataset of glycan-binding proteins was analyzed using GlyVicinity at a redundancy level of 70%. The diagrams provide information about the deviation (as a percentage, please compare with Figure 3b) from the natural abundance for amino acid residues in the vicinity of sulfated ligands.

the sulfate group is linked to uronic acid.[29,30] Uronic acid is also present in various algae saccharides (e.g. in the brown algae *Saccharina latissima*, previously described as *Laminaria saccharina*).[31] Especially in algae saccharides, we find uronic acids and sulfated saccharides as building blocks and functional groups.[31,32] Arginine and asparagine are overrepresented, as well as the aromatic residues tyrosine and tryptophan, when uronic acids are bound to the carbohydrate recognition domain (CRD) of their respective receptors (Figure 4b). Our data mining approach, applied to all sialic acid receptors and receptors of uronic acid and sulfated saccharides in the PDB, showed that the amino acid residues discussed here are essential for the specificity of receptor binding. When polySia receptors are discriminated from those with specificity for sulfated saccharides, crucial amino acid residues are determined.

Biophysical and biochemical experiments

When looking at characteristic regions of the two-dimensional (2D) NMR spectra in Figure 5 (F2 between 9 and 7 ppm, and F1 between 3 and 1.5 ppm), it is clear that the addition of polySia to the MARCKS-ED peptide causes spectral changes, suggesting that protons from the MARCKS-ED peptide are involved in binding with polySia. As shown in Figure 5a, interaction of MARCKS-ED with polySia led to disappearance of the amide signals in the 2D NMR spectrum of the complex (yellow) at 7.54 ppm. This result was accompanied by the emergence of a new set of peaks at 7.95 ppm, as well as a change in chemical shifts between the amide signals at 8.12 ppm and

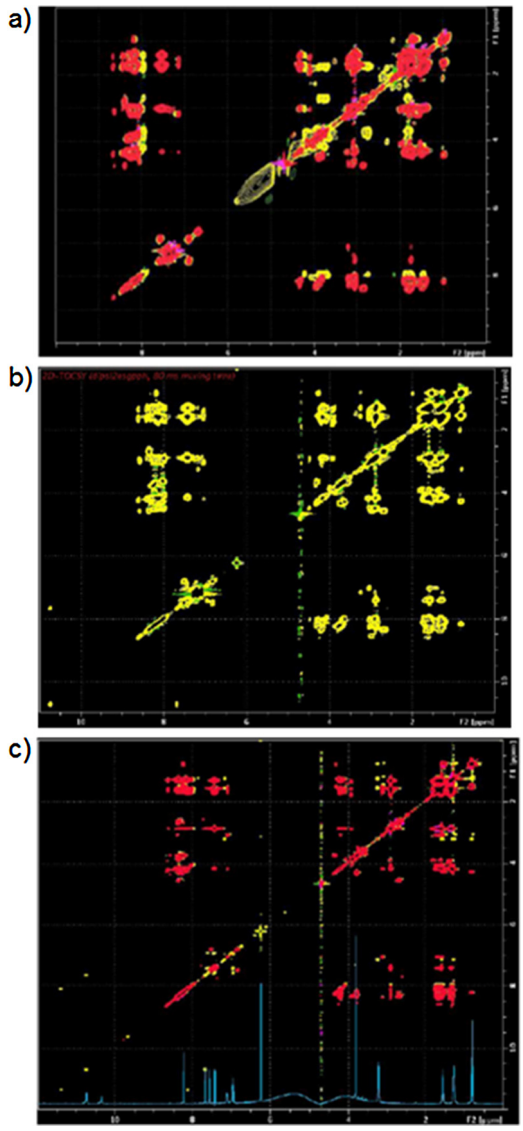

Figure 5. a) Overlay of the characteristic regions of two total correlation spectroscopy (TOCSY) spectra, indicating the interaction between polySia and the effector domain of the MARCKS-ED (KKKKKRFSFKKSFKLSGFSFKKNKK) peptide by alterations of specific ^{1}H NMR signals of amino acid residues from the MARCKS-ED. Red signals indicate the free, non-ligand-bound state, and yellow signals indicate the polySia-bound state of the MARCKS-ED. The disappearance and shifting of characteristic (yellow) cross-peaks in the bound state argues in favor of a strong participation of specific amino acid residues in ligand binding. b) MARCKS-ED in complex with tegaserod. c) MARCKS-ED control peptide (KKKKKRASAKKSAKLSGASAKKNKK) in complex with tegaserod. Red signals indicate the free, non-ligand-bound state, and yellow signals indicate the tegaserod-bound state of the MARCKS-ED control peptide. The 1D NMR spectrum on the bottom of the 2D TOCSY spectrum shows tegaserod in its free state. The strongest binding effects were detected for MARCKS-ED interacting with polySia (panel a).

8.31 ppm. Due to intermolecular exchange processes, characteristic cross-peaks disappeared in total correlation spectroscopy (TOCSY) spectra of the MARCKS-ED–polySia complex. Interaction of MARCKS-ED with the polySia mimicking compound tegaserod ((*Z*)-but-2-enedioic acid; 1-[[(*Z*)-(5-methoxyindol-3-ylidene)methyl]amino]-2-pentylguanidine)[33] led to only minor changes at these ppm values. These results argue in favor of

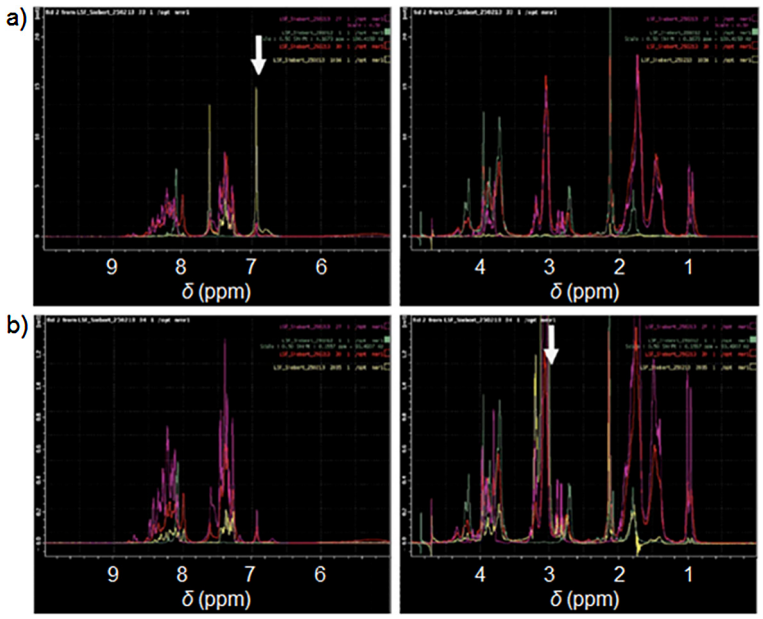

Figure 6. Saturation transfer difference (STD) NMR experiment with MARCKS-ED and polySia. a) Irradiation of a proton signal at 6.9 ppm (from protein Phe/Asn side chains). Irradiation is indicated by white arrows. Yellow: STD, red: MARCKS-ED–polySia (colominic acid) complex, green: free polySia (colominic acid), purple: free MARCKS-ED. b) Irradiation at 3.1 ppm (MARCKS-ED Lys side chain). Yellow: STD, red: MARCKS-ED–polySia (colominic acid) complex, green: free polySia (colominic acid), purple: free MARCKS-ED. The data suggest that irradiation of MARCKS-ED signals at 6.9 ppm influences the intensities of the peptide and all polySia signals at 8.0, 4.0, 3.9, 3.7, 2.1 ppm. Also, irradiation at 3.1 ppm results in an STD response to both polySia and MARCKS-ED signals, in this case predominantly, but not exclusively, to the peptide.

a weaker specific binding of the polySia mimicking molecule (Figure 5b) in comparison with the interaction with polySia fragments from colominic acid (CA). Data suggest that irradiation of MARCKS-ED signals at 6.9 ppm influenced the intensities of the peptide and all polySia signals at 8.0, 4.0, 3.9, 3.7, and 2.1 ppm (Figure 6a). Also, irradiation at 3.1 ppm resulted in a saturation transfer difference (STD) response to both polySia and MARCKS-ED signals, in this case predominantly, but not exclusively, to the peptide (Figure 6b and Supporting Information, Figure S4). These STD NMR results can therefore be used to establish a proper reference system for determining the impact of serine, arginine, and aromatic amino acid residues on binding to polySia fragments. Receptor binding of tegaserod with the control peptide did not lead to any spectral changes in these areas (no shifting or disappearing cross-peaks were observed; Figure 5c).

To further understand molecular details of the polySia receptor interaction processes, additional nuclear Overhauser effect spectroscopy (NOESY), TOCSY, and STD NMR experiments needed to be carried out for other sialic acid receptors with potential polySia affinity. Toward this aim, we also performed NMR experiments with lectin SHL-1 from the venom of the Chinese bird hunting spider *Selenocosmia huwena* Wang and with a mixture of the defensins HNP 1, 2 and 3. These data were used as a further reference to evaluate our NMR data of the linear 25-mer peptide MARCKS-ED in the absence and presence of polySia. The results of TOCSY (Figure 7) and STD (Figure 8) NMR experiments of polySia fragments with the spider lectin SHL-1 argue in favor of specific carbohydrate–protein interactions, as distinct SHL-1 NMR signals were affected. There were only a few signal alterations detected when comparing the SHL-1 TOCSY spectrum in the free state with that of the polySia-bound state (Figure 7).

To further evaluate these findings, we also performed STD NMR experiments that document an involvement of tryptophan residues in the binding process. The NMR results for the spider lectin SHL-1 in its ligand-free state, in comparison with SHL-1 interacting with a dimeric polySia fragment, were in agreement with the model description displayed in Figure 9a, which highlights three tryptophan residues (Trp 23, Trp 25, and Trp 32) critical for binding. Another suitable sialic acid mini-receptor is the human neutrophil α-defensin HNP 2.

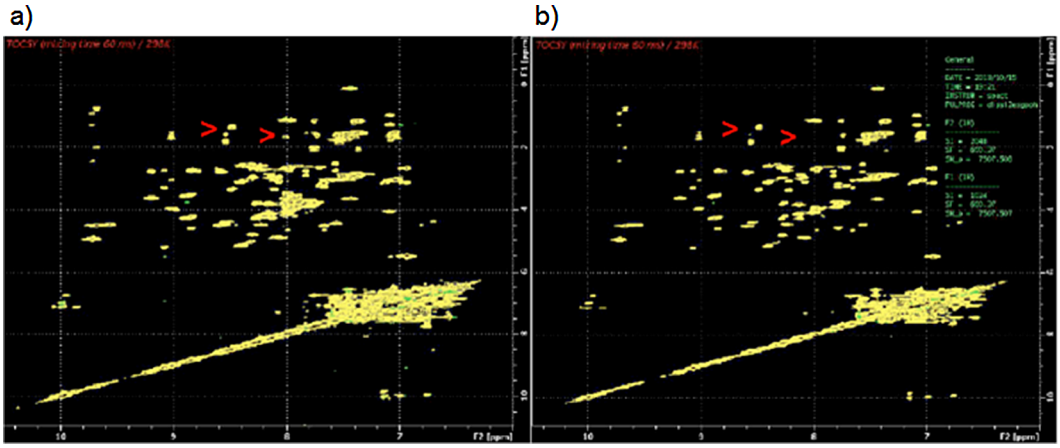

Figure 7. Two TOCSY NMR spectra indicating the interaction between polySia and the lectin from the venom of the Chinese bird-hunting spider *Selenocosmia huwena* Wang (SHL-1) by alterations of specific ^{1}H NMR signals of amino acid residues from SHL-1. a) Free, non-ligand-bound state and b) polySia-bound state of SHL-1. Signal alterations are highlighted by red arrowheads.

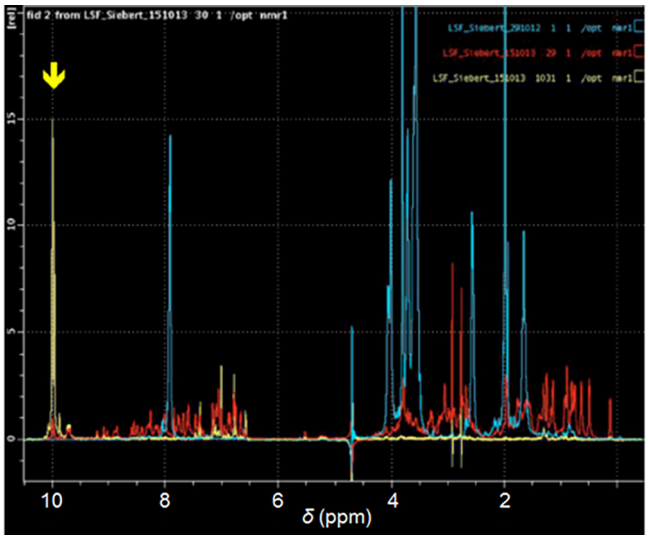

Figure 8. STD NMR experiments of SHL-1 and polySia. Yellow: STD spectrum of the lectin from the venom of the Chinese bird-hunting spider *S. huwena* Wang (SHL-1) in complex with polySia fragments; (red: free SHL-1, blue: free polySia fragments from colominic acid; yellow: SHL-1–polySia (colominic acid) complex). Irradiation is indicated by a yellow arrow at 10 ppm.

Defensins are small (18- to 45-residue) cationic peptides that are carbohydrate-binding lectins and possess antimicrobial properties. As displayed in Figure 9b, the amino acid residues relevant for binding were Tyr 2, Arg 4, Tyr 20, and Trp 25. Finally, as is also the case for the human α-defensins under study, a number of distinct signal alterations of characteristic amino acid residues were detected in a similar way as was possible when MARCKS-ED spectra were compared in the absence and presence of polySia fragments. NMR experiments using SHL-1 or the human α-defensins HNP 1, 2, or 3 as receptors and polySia fragments from CA as ligands revealed that three aromatic amino acid residues and an arginine residue play a major role in carbohydrate binding (Figure 9). As the MARCKS-ED also comprises the aromatic amino acid (Phe), we turned our attention to the interaction of polySia with arginine, phenylalanine, and serine in the MARCKS-ED. In this context, the strategic combination of methods led to new insight into molecular neurosciences, providing data that explained why bioactive compounds like cyclic and linear peptides or small organic molecules, especially polar molecules with partially equalized single and double bonds, can act as glycomimetics.[29,35–37] The polySia mini-receptors used in this study were derived from structural models of SHL-1,[25] as well as NMR and X-ray models from α-defensins HD5 and HNP 1, 2, and 3.[38–42] A combination of molecular dynamics docking simulations with ab initio calculations of the small organic glycomimetic molecules provided detailed information about the fine-tuning of such binding processes.

For example, it was possible to determine stable binding modes of the sialic acid mini-receptor HD5 with *cis*- as well as with *trans*-tegaserod (Figure 10a). Four low-energy states (I–IV)

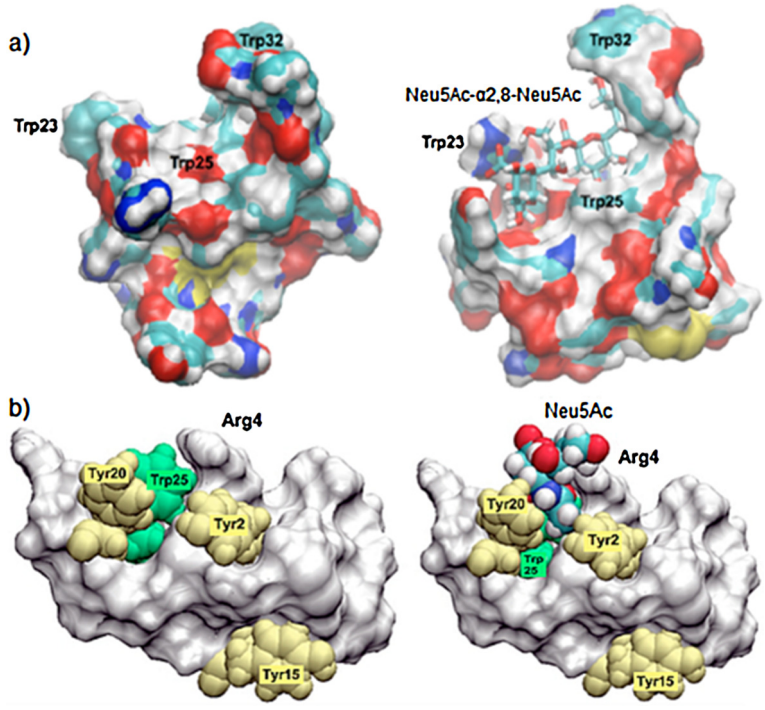

Figure 9. a) Surface representation of the lectin SHL-1 from the Chinese bird-hunting spider *S. huwena* Wang in the ligand-free state (left) and in complex with a polySia disaccharide fragment (right). Three tryptophan residues (Trp 23, Trp 25, and Trp 32) are indicated, all of which are involved in ligand binding. The images show the shape of a sialic acid binding pocket that is the length of two disaccharide units. In contrast to residues Trp 23 and Trp 25, which are essential for complex formation, the Trp 32 residue stabilizes the complex, but is not essential for specific ligand binding. b) Surface representation of the human α-defensin HNP2 in the absence (left) and presence (right) of a sialic acid ligand. The amino acids relevant to binding are: Tyr 2, Arg 4, Tyr 20, and Trp 25. The ligand-free state corresponds to the NMR structure (PDB ID: 1QK7) published in 1999.[81]

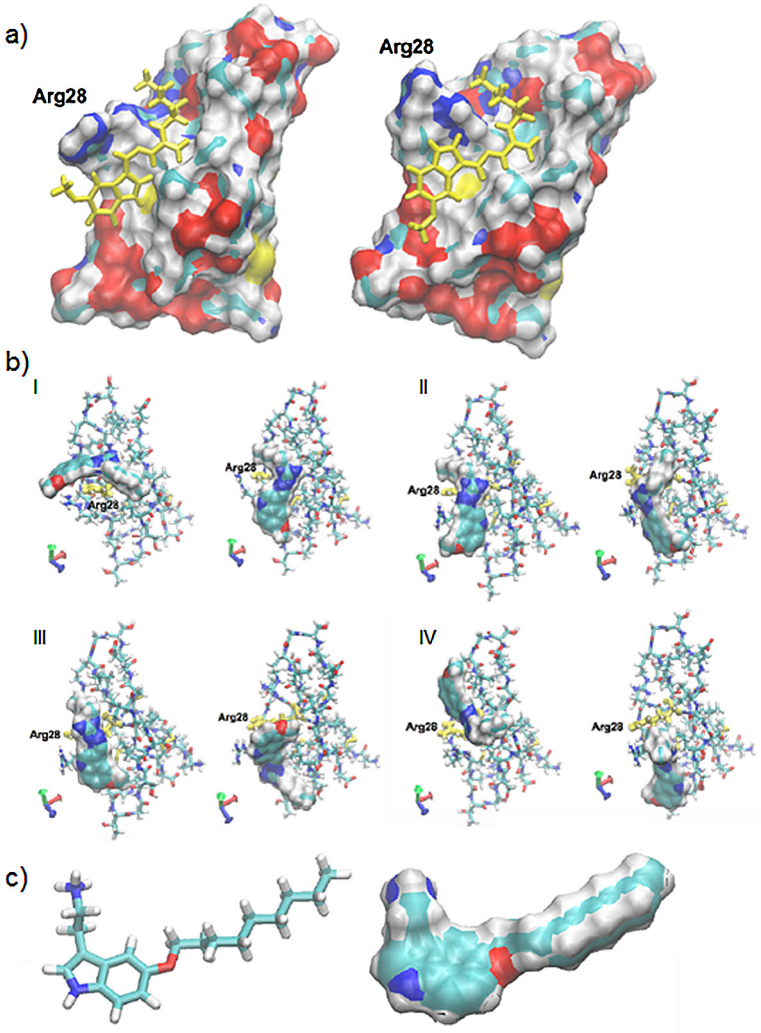

Figure 10. a) *cis*-Tegaserod (left) and *trans*-tegaserod (right) in complex with a sialic acid specific mini-receptor, the α-defensin HD5. b) Lowest energy states (I–IV) of *cis*-tegaserod (left) and *trans*-tegaserod (right) in complex with α-defensin HD5. Four low-energy complexes with *cis*-tegaserod are presented at left. Four corresponding low-energy complexes with *trans*-tegaserod are shown at right. Both configurations started at the lowest energy state (I). The maximum energy difference between *cis*-tegaserod–HD5 complexes I and IV is 7.2 kcal mol^{-1}. The maximum energy difference between *trans*-tegaserod–HD5 complexes I and IV is 5.6 kcal mol^{-1}. At least one arginine residue (Arg 28) in all energy-minimum conformations is involved in complex stabilization. c) Density functional theory (DFT) calculation of nonyloxytryptamine in water; presentation of the energy minimum conformation in the free state. Stick model is shown at left; space-filling surface low-energy structure is presented at right.

of *cis*-tegaserod and *trans*-tegaserod, each in complex with the α-defensin HD5, are displayed in Figure 10b. As defensins are cationic antimicrobial peptides, arginine residues are important contact points to initiate ligand binding. At least one arginine residue stabilizes the receptor–ligand complex, and in all cases, Arg 28 is involved as a crucial residue. The maximum energy difference between the *cis*-tegaserod–HD5 complex states I–IV was 7.2 kcal mol^{-1}, as revealed by molecular docking simulations. The maximum energy difference between the *trans*-tegaserod–HD5 complex states I–IV was 5.6 kcal mol^{-1}, according to the corresponding calculations.

These values can be used for the determination of a statistical abundance distribution of the adopted HD5–tegaserod complexes. α-Defensins such as HD5 and HNP 1, 2, and 3 bind to sialic acids, as indicated by the results from NMR and SPR experiments carried out during this study with these α-defensins, derived from psoriatic skin cells and various sialic acids. The crucial amino acid residue for Neu5Ac, as well as for tegaserod binding, was Arg 28 of HD5, as highlighted in Figure 10b (see also higher-magnification images in the Supporting Information). When determining the dissociation constant (K_D) values for HD5 and the ligands Neu5Ac or *N*-acetylmuramic acid (Mur2Ac) with SPR methods, we observed that the corresponding K_D value increased by more than 100% when the Arg 28 residue was replaced by alanine (Supporting Information, Figure S3). However, the replacement of Arg 32 by an alanine residue also led to a significant decrease in the K_D (unpublished observations). *Cis*- and *trans*-tegaserod molecules were bound by the sialic-acid-specific α-defensin HD5 with similar affinities for different orientations of the molecules. Therefore, we concluded that the overall shape of tegaserod is not the only binding criterion. Other physical parameters, such as the vibrational states of certain functional groups, which we also calculated using an ab initio approach, may be important for the creation of low energy ligand–receptor complexes. Sialic acid receptor interactions of molecules similar to tegaserod, like nonyloxytryptamine, have also been studied.[43] An energy minimized structure of this ligand, as derived from density functional theory (DFT) calculations in the framework of a molecular modeling study, is shown in Figure 10c. The shapes of nonyloxytryptamine and tegaserod are similar and differ significantly from that of polySia fragments. When comparing the structures of nonyloxytryptamine and tegaserod (Figure 10a,b vs. Figure 10c), the side chain of the pyrrole ring of the indole ring system, which influences the vibrational states of the two molecules, is the most obvious difference. It is remarkable that, in the case of nonyloxytryptamine (Figure 10c), an oxygen atom is present instead of a carbon atom, which is also responsible for remarkable differences in structural dynamics, as analyzed previously for other examples and described in the literature.[36] The deviations between these polySia mimetics and polySia itself are similar to those between HNK-1 and certain cyclic peptides, as described.[29] Therefore, we can conclude that, in addition to structural criteria, additional dynamic parameters are crucial for receptor binding, such as vibrational states,[44] which can be determined with the help of quantum chemical ab initio calculations.

The findings outlined above are of importance for therapeutic improvements in the field of nerve cell regeneration, as we provide here a submolecular description of why *cis*- and *trans*-tegaserod, or similar molecules like nonyloxytryptamine, can

act as polySia glycomimetic molecules, similar to polySia fragments of various lengths. Previously, evidence was found that tegaserod treatment enhances regeneration after femoral nerve injury and spinal cord injury in mice.[33,34] We will use these results for new clinical strategies to solve medical problems related to nerve cell regeneration processes as well as the problem of malignancy of neuronal tumors, as described in detail below. Our NMR and molecular modeling studies have also proven to be extremely helpful when sulfated polysaccharides need to be analyzed in molecular detail. These polysaccharides might be an important addition in the fine-tuning of new therapeutic approaches related to polySia or polySia mimetics because they are able to block migration of tumor cells.

As the analyzed sulfated polysaccharides from algae were mixtures of saccharides of different sizes, it was necessary that, in addition to the TOCSY and NOESY experiments, diffusion-ordered spectroscopy (DOSY) measurements were also carried out. DOSY spectra of two different polysaccharide samples from brown and green algae, as well as of CA (*E. coli*-derived polySia fragments) are shown in the Supporting Information (Figure S1 a,b,c). The polysaccharides studied can contain up to 100 monosaccharide residues. However, shorter fragments are preferable in solution. In all cases, linear polysaccharide fragments were only two to three residues in length, due to the sizes of the receptor binding pockets. Green algae contain sulfuric acid polysaccharides, sulfated galactans, and xylans. Brown algae incorporate alginic acid, fucoidan (sulfated fucose), laminarin (β-1,3 glucan), and sargassan (a sulfated heteropolysaccharide comprising D-glucuronic acid, D-mannose, D-galactose, D-xylose, and L-fucose residues).[31] DOSY experiments are suitable to determine the size distribution of compounds in a complex mixture. Values concerning the size distribution and the diffusion constants, which we obtained from the DOSY NMR experiments, indicated that these two algae polysaccharide mixtures were nearly identical (Supporting Information, Figure S1). The structural role of sulfation in saccharides has already been analyzed with molecular modeling tools, including ab initio calculations, in a previous study.[38] It was shown that sulfate groups are special contact points for a receptor but can also influence the conformation of the polysaccharide.

PolySia cleavage and tumor cell differentiation

A number of studies have shown that polySia is overexpressed in many tumors, such as malignant gliomas, small cell lung cancer, and neuroblastomas, to name a few.[18,45–52] It has been postulated that polySia enables tumor cells to remain in an undifferentiated state and therefore to exist outside of the cellular "social network" and grow irrespective of regulating factors expressed by the neighboring cells. Also, the characteristic polySia function, to accelerate migration of stem cells,[18,46–51] is used by tumor cells to infiltrate normal tissue and metastasize.[18] PolySia can act as ligand for certain receptors or as an NCAM interaction inhibitor.[11,20] The second scenario means that different pathways induced by NCAM activation can be blocked by the expression of polySia on NCAM. A model of

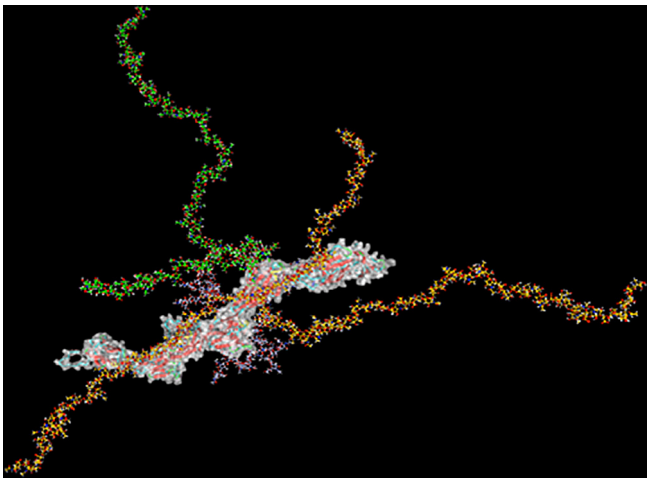

Figure 11. PolySia–NCAM-140 model generated from a published in silico dataset.[9a] A homology model of NCAM-140 was calculated with Modeller.[9b] Complex-type glycan chains were added with GlyProt[9c] to N-glycosylation sites N222, N315, N347, N423, N449, and N478. Based on characterization of the polysialylation status of NCAM in postnatal mouse brains, the glycan chain at position N449 (green) contains two polySia chains consisting of 38 and 20 sialic acid residues. The *N*-glycan chain at position N478 (orange) carries three polySia chains of 38, 30, and 20 sialic acid residues. No polySia residues were added to the remaining *N*-glycans (purple). The image was created with YASARA.[9d]

NCAM with its polySia chains is shown in Figure 11. For example, NCAM interacting with integrin on the cell surface initiates the differentiation of neuroblastoma cells. The presence of polySia on NCAM inhibits this interaction[53–56] and prevents tumor cells from differentiating. Pax3, which is a transcription factor involved in tumorigenesis, seems to induce NCAM polysialylation on medulloblastoma cells.[57] PolySia inhibits cell–cell interactions through its ability to bind a significant amount of water and therefore keeps receptors away from their ligand or other receptors. Some studies postulate that polySia expression on tumor cells can be used as a prognostic factor for tumor malignancy and severity of the disease outcome. Wilms tumor patients with increased polySia expression, for example, have a shorter survival time; therefore, polySia was claimed to be an oncodevelopmental antigen.[58,59] It should be considered here that such alterations at the glycocalix may have a significant impact on the physical properties of a cell, which are related to their motility.[60]

In addition to using polySia as a prognostic marker in tumors, there is also a therapeutic approach with respect to tumors through cleavage of polySia from the surface of polySia-expressing tumor cells. Endo N is a selective polySia-cleaving enzyme. PolySia cleavage on the surface of human SH-SY5Y neuroblastoma cells with the nontoxic endo N induced differentiation of these cells and led to development of axons and expression of neurofilaments (Figure 12). Additionally, the migration capacity of these cells was shown to be significantly decreased when they were treated with endo N.[61,62] Unfortunately, in vivo experiments with intravenous application of endo N in animals with polySia-rich tumors failed to remove

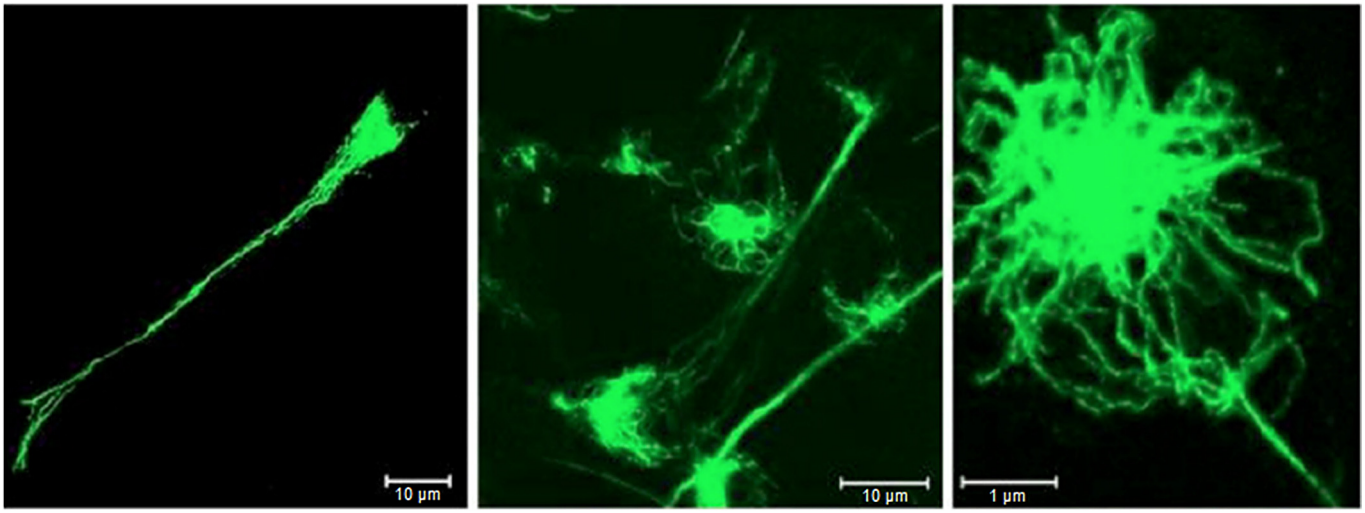

Figure 12. Intermediate neurofilament (NF-M) expression in human SH-SY5Y cells treated with endoneuraminidase N. The neuroblastoma cells which were treated with endoneuraminidase N not only phenotypically developed axons, but also expressed neurofilament M (intermediate). The green staining of neurofilament M indicates that cells differentiate into neuronal cells when observing and documenting this process after certain time steps. The neuroblastoma cells shown in this figure belong to the same cell cluster. Scale bars: 1 µm (right image) and 10 µm (middle and left image). The magnification was (from left to right) 1200×, 2000×, 5000× using a Zeiss confocal microscope.

polySia from the tumor cells, due to serum factors that inactivated endo N (unpublished observations). Therefore, alternative delivery methods for endo N to tumors have to be evaluated. However, the cleavage of polySia from tumor cells could be a promising tool in the treatment of cancer.

As we have found that sulfated polysaccharides of algae origin are able to block neuronal cell migration (Figure 13), the application of these molecules could also support an antitumor therapy and will be analyzed in a follow-up study. Furthermore, the sulfated polysaccharides studied have a concentration-dependent influence on neurite outgrowth, which we have tested also in combination with certain collagen fragments (Supporting Information, Figure S2). Compared with control cells grown on the neutral substrate poly-L-lysine, the sulfated polysaccharides from algae show a statistically significant enhancement of neurite outgrowth at concentrations from 0.0001 to 0.1 mg mL^{-1}. However, at concentrations that were higher than 1 mg mL^{-1}, the sulfated polysaccharides exhibited inhibitory effects on neurite outgrowth. Therefore, the sulfated polysaccharides from mixtures of brown and green algae, with or without bioactive collagen fragments, can also be applied in addition to polySia or polySia mimicking molecules when lesions in neuronal tissues need to be cured.[63–66]

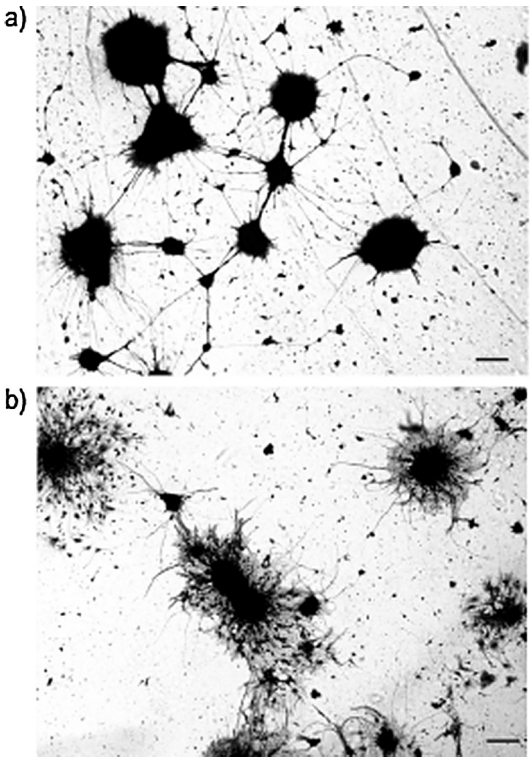

Figure 13. Impact of sulfated polysaccharides from brown and green algae[31] on the migration of primary neurons from cerebellar explants. Representative images show explants cultured on a) sulfated polysaccharides from brown and green algae, or b) control substrate poly-L-lysine. Sulfated polysaccharides strongly inhibited cerebellar neuron migration. The scale bars at the lower right of each image correspond to 100 µm. Various concentrations (1 µg mL^{-1} to 5 mg mL^{-1}) were used, as was the case for testing neurite outgrowth (see Supporting Information, Figure S2 a).[82] The migration of neurons from the explant core was analyzed 48 h after seeding. An exemplary figure documenting neurite outgrowth in the presence and absence of collagen fragments is given in the Supporting Information (Figure S2 b).

Induced polySia expression in glial scar tissue after spinal cord lesion

In addition to an important biomedical role in neurooncology, polySia–receptor interactions, as described here for various model systems, are also of particular clinical interest when neuronal regeneration processes have to be supported by innovative drugs for therapeutic reasons. In both cases (tumor growth and scar development after injuries in which nerve cells are involved), a high concentration of polySia on the cell

surfaces corresponds to de-differentiation processes that must be considered in each therapeutic approach. These findings are independent of the lengths of the various glycan chains that are occurring on the cell surfaces. The ability of polySia expressing cells to maintain their distance from other cells inspired work on a cell regeneration experiment in which polySia expression in astroglia was induced to inhibit the barrier of scar tissue after spinal cord lesions.[61] It was shown that retrovirally induced polySia overexpression in astroglia, which formed the spinal cord scar, rendered the glial scar permeable for regrowing spinal cord axons.[61] Furthermore, application of polySia mimicking peptides led to better functional recovery after spinal cord injury and to decreased reactive gliosis.[67,68] These are important experiments, demonstrating that spinal cord axons have the ability to grow but cannot pass the glial scar unless the scar tissue is made permeable. For the first time, penetration of the scar tissue and growth of a satisfactory number of axons distal to the scar could be observed in these studies.[61]

Conclusions

Although the results presented here are very promising, there is a major obstacle that has to be solved with the support of nanomedical techniques in near future. Previous studies using polySia-overexpressing cells or virally induced polySia expression proved that the gliosis is not a barrier that will never be broken, as Cajal stated in 1928.[69] However, the induced overexpression of polySia through retroviral delivery of this macromolecule in humans is not free of risk and could possibly have adverse effects. Other methods of polySia expression in a glial scar have to be developed which are safer for use in human beings. In this case, the expression of polySia in glial scars could become a milestone in the central nervous regeneration of spinal cord injuries when all interactions are understood on a submolecular level. Fragments of polySia, as well as polySia mimetics like tegaserod and nonyloxytryptamine, could also play a crucial role in this context,[33,34,67,68,70] due to their strong impact on neuronal outgrowth and migration. It is important to mention that polySia is not oncogenic. It is expressed by tumor cells, but there are no observations that it induces cancer.

The high clinical relevance with respect to the therapy of diseases associated with neuronal regeneration, tumor spread, and infection[71] opens a wide field for medical and pharmacological research projects related to polySia and polySia glycomimetic molecules. Sulfated polysaccharides of different origins (e.g., from green and brown algae) are well-suited to support these new therapeutic approaches. Sulfated polysaccharides mainly interact with arginine and tyrosine residues in the receptor binding pocket in a similar way to sialic acids. The most prominent binding partners that stabilize sialic acid–protein complexes are tryptophan, tyrosine, and arginine residues. This is also the case for polySia glycomimetics. Sulfated polysaccharides of algae origin are able to block neuronal cell migration. It is now possible to identify certain functional groups and correlate their interactions with biological effects. Sulfate groups of algae polysaccharides, as well as the *N*-acetyl group and the carboxyl group, together with hydroxy groups of sialic acid residues, are essential for stable binding with crucial amino acids (e.g., arginine, tyrosine, and tryptophan) on the receptor side. As shown in Figure S3 a–d (Supporting Information), when using the α-defensins HNP 2 and HD5 as sialic acid mini-receptor models, the carboxylic group is particularly essential for a specific and stable ligand–receptor interaction. Tegaserod and 5-nonyloxytryptamine, as polySia glycomimetic molecules, fit their aromatic ring systems in the corresponding binding pockets of sialic acid receptors. In Figure S4 a and b (Supporting Information), it is shown that the involvement of the aromatic ring system of tegaserod can already be documented by one-dimensional (1D) ^{1}H NMR experiments. The interactions between the MARCKS-ED peptide and SHL-1 with polySia were confirmed and explained on a submolecular level by combining NMR and in silico studies. We identified general binding principles for the interactions of MARCKS-ED peptide, SHL-1, and α-defensin with their respective carbohydrate or glycomimetic binding partners.

It should not be surprising that various diseases of different origin can be treated with drugs based on such insight, because these saccharides or their glycomimetics have to be considered as the essential contact structures on the cell surface.[72] We conclude that polySia, polySia glycomimetic molecules, and sulfated polysaccharides are feasible for clinical applications but need to be further analyzed on a nanoscale level, as described herein, in order to understand their interactions with other molecules in detail for optimal application in the corresponding therapies. Particularly when these molecules interact with certain receptors and impact nerve cell differentiation as well as tumor spread, the interactions must be fully describable in relation to various cell biological processes in order to improve such therapies.

Experimental Section

Materials: KKKKKRFSFKKSFKLSGFSFKKNKK and the corresponding control peptide KKKKKR**A**S**A**KKS**A**KLSG**A**S**A**KKNKK; (sequence differences are in bold) were purchased from Schafer-N (Copenhagen, Denmark). The polySia probes originated from colominic acid (CA). The α-defensins HNP 1, 2, and 3 were derived from psoriatic skin cells and isolated as published.[73]

Cell culture and treatment of SH-SY5Y neuroblastoma cells: SH-SY5Y neuroblastoma cells (ATCC, Rockville, MD, USA), which are rich in polySia expression, were plated on glass coverslips and cultivated in Dulbecco's modified Eagle's medium (DMEM)/Ham's F12 (1:1; Fisher Scientific) on a nanoscale level, as previously described.[47] When cells reached a confluency of ~60% (change of medium every 3 days), 6–8 U mL^{-1} of endoneuraminidase N (endo N; gift from Dr. Urs Rutishauser, Memorial Sloan Kettering Cancer Center [MSKCC], NY, USA) were added, and 24–48 h after addition of endo N, cells were fixed and prepared for immunostaining.[47] The complete removal of polySia was verified as described using polySia-specific antibodies.[47]

Staining of SH-SY5Y cells: Cells were fixed in 4% paraformaldehyde at 2 h and 4 °C as described, permeabilized, and stained for polySia using mouse monoclonal polySia-specific antibody 5A5

(1:1000; gift from Dr. Urs Rutishauser) or stained for neurofilament expression using a primary mouse antibody directed against neurofilament M (1:200; Sigma–Aldrich, St. Louis, MO, USA). Cells were incubated with primary antibody overnight at 4 °C, and after several washes with phosphate-buffered saline (PBS) solution, Cy3-conjugated secondary antibody (1:100; Jackson ImmunoResearch, West Grove, PA, USA) was applied for 1 h at room temperature. Coverslips were washed again and mounted using an anti-fading mounting solution (gift from Dr. El-Maarouf, MSKCC, NY, USA).[47]

NMR methods: NMR spectra were recorded on a Bruker Avance III 600 MHz UltraShield spectrometer at 298 K in 10% D_2O. TOCSY and NOESY spectra were recorded using standard pulse programs,[74,75] with mixing times of 80 ms and 200 ms, respectively. The molar ratio of polySia to the receptor peptides was 5:1 for these NMR experiments. The STD NMR experiments were performed as described[28,76] using a 10:1 ligand/receptor molar ratio for the interaction experiments, with 0.5, 1, and 2 s saturation times (by concatenation of 50 ms Gaussian pulses separated by 1 ms).

Molecular modeling / docking study: The 3D structure of *Selenocosmia huwena* Lectin-I (SHL-1) from the venom of the spider *S. huwena* Wang was taken from the PDB (PDB ID: 1QK7).[81] Docking studies were performed with the AutoDock 4.2 software, which uses the Lamarckian genetic algorithm (LGA). For docking of the polySia disaccharide fragment with SHL-1, the required file for the ligand was created by the AutoDock 4.2 software package. The grid size was set to 126, 126, and 126 Å along the *x*-, *y*-, and *z*-axes. In order to recognize the binding site of the polySia disaccharide in SHL-1, a blind docking simulation was adopted. The docking parameters used were as follows: GA population size = 150; maximum number of energy evaluations = 250 000. The lowest binding energy conformer was taken from 10 different conformations for each docking simulation, and the resulting minimum energy conformation was applied for further analysis. The PyMOL software package was used for visualization of the docked complex.[77]

Mouse studies: C57BL/6J mice of either sex were used as wild-type mice. Mice were kept under standard laboratory conditions with food and water supply ad libitum and with an artificial 12 h light/dark cycle. All experiments were conducted in accordance with the German and European Community laws on protection of experimental animals, and all procedures used were approved by the responsible committee of the State of Hamburg. This paper was written in compliance with the ARRIVE guidelines for reports on animal research.

Neuronal culture and neurite outgrowth: Cerebellar granule neurons were used as archetype neurons and prepared from the cerebella of six- to eight-day-old wild-type mice and cultured in defined serum-free medium composed of Neurobasal A medium (Invitrogen, Thermo Fisher Scientific), supplemented with 1 mM L-glutamine (Invitrogen), 0.5% (*v*/*v*) B27 (Invitrogen), 100 μg mL^{-1} holotransferrin (Merck Chemicals, Darmstadt), 10 μg mL^{-1} insulin (Sigma–Aldrich), 30 nM sodium selenite (Sigma–Aldrich), and 4 nM L-thyroxine (Sigma–Aldrich), as previously described.[76] Neurons were seeded at a density of 2.5×10^4 cells per well in 48-well plates (Sarstedt, Numbrecht, Germany) coated with poly-L-lysine (PLL; Sigma–Aldrich) or with varying concentrations of glycans (special mixture from Ocean Harvest Ltd., 1 μg mL^{-1} to 5 mg mL^{-1}), alone or in combination with collagen hydrolysates of fish or pig origin. Neurite length was measured after 24 h, as previously described, using an Axiovert 135 microscope equipped with AxioVision 4.6 software (Carl Zeiss, Oberkochen).[78] In each experiment, at least 50 cells on each of two coverslips were analyzed, and the total neurite length was determined by measuring the length of all neurites per cell that were longer than the cell body. The results of three independent experiments were averaged.

Microexplant culture and neuronal migration: Microexplant cultures from cerebella of six- or seven-day-old wild-type mice were prepared as described.[79,80] Cerebellar explants were cultured on PLL or glycans at 1 μg mL^{-1} to 5 mg mL^{-1} concentration in the same medium stated above, supplemented with 10% horse serum and 10% fetal calf serum. After 16 h in culture, the medium was changed to serum-free medium, and the explants were cultured for an additional 32 h. After 48 h, in vitro explants were fixed with glutaraldehyde, stained with toluidine blue/trypan blue, and imaged using an Axiovert 135 microscope equipped with AxioVision software 4.6 (Carl Zeiss).

Statistics: Differences between groups in the neurite outgrowth assay were determined by the two-tailed *t*-test. Results are expressed as mean ± SEM; $p < 0.05$: statistically significant for all statistical tests.

Acknowledgements

The authors thank Philipp Siebert for technical assistance and Eva Kronberg for the excellent care of animals. Elements of the project were financed by the European Commission's Framework Program 7 (Bio-NMR; project number 261863). The authors also thank their colleagues, H. Maximilian Mehdorn, Robert I. Lehrer, and Wuyuan Lu for many fruitful discussions, and the Sialic Acids Society of Kiel for financial support.

Keywords: molecular interactions · polysia mimetics · polysialic acid · sulfated polysaccharides

[1] R. Schauer, *Curr. Opin. Struct. Biol.* **2009**, *19*, 507 – 514.
[2] M. D. Battistel, M. Shangold, L. Trinh, J. Shiloach, D. I. Freedberg, *J. Am. Chem. Soc.* **2012**, *134*, 10717 – 10720.
[3] C. Sato, K. Kitajima, *Front. Cell. Neurosci.* **2013**, *7*, 61.
[4] M. Rollenhagen, S. Kuckuck, C. Ulm, M. Hartmann, S. P. Galuska, R. Geyer, H. Geyer, M. Mühlenhoff, *J. Biol. Chem.* **2012**, *287*, 35170 – 35180.
[5] H. Hildebrandt, A. Dityatev, *Top. Curr. Chem.* **2013**, *366*, 55-96.
[6] *Sialobiology: Structure, Biosynthesis, and Function* (Eds.: J. Tiralongo, I. Martinez-Duncker), Bentham Science, Oak Park, **2013**.
[7] R. Schauer, *Zoology* **2004**, *107*, 49 – 64.
[8] P. Simon, S. Bäumner, O. Busch, R. Röhrich, M. Kaese, P. Richterich, A. Wehrend, K. Müller, R. Gerardy-Schahn, M. Mühlenhoff, H. Geyer, R. Geyer, R. Middendorff, S. P. Galuska, *J. Biol. Chem.* **2013**, *288*, 18825 – 18833.
[9] a) C. Ulm, M. Saffarzadeh, P. Mahavadi, S. Müller, G. Prem, F. Saboor, P. Simon, R. Middendorff, H. Geyer, I. Henneke, N. Bayer, S. Rinné, T. Lütteke, E. Böttcher-Friebertshäuser, R. Gerardy-Schahn, D. Schwarzer, M. Mühlenhoff, K. T. Preissner, A. Günther, R. Geyer, S. P. Galuska, *Cell. Mol. Life Sci.* **2013**, *70*, 3695 – 3708; b) N. Eswar, B. Webb, M. A. Marti-Renom, M. S. Madhusudhan, D. Eramian, M. Y. Shen, U. Pieper, A. Sali, *Curr. Protoc. Bioinformatics* **2006**, Ch. 5, Unit 5.6, DOI: 10.1002/0471250953.bi0506s15; c) A. Bohne-Lang, C. W. von der Lieth, *Nucleic Acids Res.* **2005**, *33*, W214 – W219; d) E. Krieger, K. Joo, J. Lee, J. Lee, S. Raman, J. Thompson, M. Tyka, D. Baker, K. Karplus, *Proteins: Struct. Funct. Bioinf.* **2009**, *77*, 114 – 122.
[10] B. Mishra, M. von der Ohe, C. Schulze, S. Bian, T. Makhina, G. Loers, R. Kleene, M. Schachner, *J. Neurosci.* **2010**, *30*, 12400 – 12413.

[11] T. Theis, B. Mishra, M. von der Ohe, G. Loers, M. Prondzynski, O. Pless, P. J. Blackshear, M. Schachner, R. Kleene, *J. Biol. Chem.* **2013**, *288*, 6726 – 6742.
[12] Y. Kizuka, S. Oka, *Cell. Mol. Life Sci.* **2012**, *69*, 4135 – 4147.
[13] S. R. Haseley, H. J. Vermeer, J. P. Kamerling, J. F. G. Vliegenthart, *Proc. Natl. Acad. Sci. USA* **2001**, *98*, 9419 – 9424.
[14] K. Nishiyama, Y. Takakusagi, T. Kusayanagi, Y. Matsumoto, S. Habu, K. Kuramochi, F. Sugawara, K. Sakaguchi, H. Takahashi, H. Natsugari, S. Bioorg, *Med. Chem.* **2009**, *17*, 195 – 202.
[15] M. Kilcoyne, J. Q. Gerlach, R. Gough, M. E. Gallagher, M. Kane, S. D. Carrington, L. Joshi, *Anal. Chem.* **2012**, *84*, 3330 – 3338.
[16] U. Rutishauser, *Nat. Rev. Neurosci.* **2008**, *9*, 26 – 35.
[17] O. Senkov, M. Sun, B. Weinhold, R. Gerardy-Schahn, M. Schachner, A. Dityatev, *J. Neurosci.* **2006**, *26*, 10888 – 109898.
[18] A. K. Petridis, H. Wedderkopp, H. H. Hugo, H. M. Mehdorn, *Acta Neurochir.* **2009**, *151*, 601 – 603.
[19] H.-C. Siebert, K. Born, S. André, M. Frank, H. Kaltner, C. W. von der Lieth, A. J. Heck, J. Jiménez-Barbero, J. Kopitz, H. J. Gabius, *Chem. Eur. J.* **2006**, *12*, 388 – 402.
[20] R. Kleene, M. Schachner, *Nat. Rev. Neurosci.* **2004**, *5*, 195 – 208.
[21] S. N. Masand, J. Chen, I. J. Perron, B. C. Hammerling, G. Loers, M. Schachner, D. I. Shreiber, *Biomaterials* **2012**, *33*, 8353 – 8362.
[22] A. Mehanna, B. Mishra, N. Kurschat, C. Schulze, S. Bian, G. Loers, A. Irintchev, M. Schachner, *Brain* **2009**, *132*, 1449 – 1462.
[23] S. Liang, *Toxicon* **2004**, *43*, 575 – 585.
[24] M. A. Rojas-Macias, T. Lütteke, *Methods Mol. Biol.* **2015**, *1273*, 215 – 226.
[25] H.-C. Siebert, S. Y. Lu, R. Wechselberger, K. Born, T. Eckert, S. P. Liang, C. W. von der Lieth, J. Jiménez-Barbero, R. Schauer, J. F. G. Vliegenthart, T. Lütteke, S. André, H. Kaltner, H. J. Gabius, T. Kozár, *Carbohydr. Res.* **2009**, *344*, 1515 – 1525.
[26] H.-C. Siebert, S. Y. Lü, M. Frank, J. Kramer, R. Wechselberger, J. Joosten, S. André, K. Rittenhouse-Olson, R. Roy, C. W. von der Lieth, R. Kaptein, J. F. Vliegenthart, A. J. Heck, H. J. Gabius, *Biochemistry* **2002**, *41*, 9707 – 9717.
[27] H.-C. Siebert, S. André, S. Y. Lu, M. Frank, H. Kaltner, J. A. van Kuik, E. Y. Korchagina, N. Bovin, E. Tajkhorshid, R. Kaptein, J. F. G. Vliegenthart, C. W. von der Lieth, J. Jiménez-Barbero, J. Kopitz, H. J. Gabius, *Biochemistry* **2003**, *42*, 14762 – 14773.
[28] V. Roldós, F. J. Cañada, J. Jiménez-Barbero, *ChemBioChem* **2011**, *12*, 990 – 1005.
[29] A. Bhunia, S. Vivekanandan, T. Eckert, M. Burg-Roderfeld, R. Wechselberger, J. Romanuka, D. Bächle, A. V. Kornilov, C. W. von der Lieth, J. Jiménez-Barbero, N. E. Nifantiev, M. Schachner, N. Sewald, T. Lütteke, G. Hans-Joachim, H.-C. Siebert, *J. Am. Chem. Soc.* **2010**, *132*, 96 – 105.
[30] Y. E. Tsvetkov, M. Burg-Roderfeld, G. Loers, A. Ardá, E. V. Sukhova, E. A. Khatuntseva, A. A. Grachev, A. O. Chizhov, H.-C. Siebert, M. Schachner, J. Jiménez-Barbero, N. E. Nifantiev, *J. Am. Chem. Soc.* **2012**, *134*, 426 – 435.
[31] S. L. Holdt, S. Kraan, *J. Appl. Phycol.* **2011**, *23*, 543 – 597.
[32] D. O. Croci, A. Cumashi, N. A. Ushakova, M. E. Preobrazhenskaya, A. Piccoli, L. Totani, N. E. Ustyuzhanina, M. I. Bilan, A. I. Usov, A. A. Grachev, G. E. Morozevich, A. E. Berman, C. J. Sanderson, M. Kelly, P. Di Gregorio, C. Rossi, N. Tinari, S. Iacobelli, G. A. Rabinovich, N. E. Nifantiev, *PLoS One* **2011**, *6*, e17283.
[33] J. Bushman, B. Mishra, M. Ezra, S. Gul, C. Schulze, S. Chaudhury, D. Ripoll, A. Wallqvist, J. Kohn, M. Schachner, G. Loers, *Neuropharmacology* **2014**, *79*, 456 – 466.
[34] H. C. Pan, Y. G. Shen, G. Loers, I. Jakovcevski, M. Schachner, *Neuroscience* **2014**, *277*, 356 – 366.
[35] J. H. van Lenthe, D. H. W. van Boer, R. W. A. den Havenith, R. Schauer, H.-C. Siebert, *J. Mol. Struct.* **2004**, *677*, 29 – 37.
[36] H.-C. Siebert, E. Tajkhorshid, J. Dabrowski, *J. Phys. Chem. A* **2001**, *105*, 8488 – 8494.
[37] T. Eckert, S. Stötzel, M. Burg-Roderfeld, J. Sewing, T. Lütteke, N. E. Nifantiev, J. F. G. Vliegenthart, H.-C. Siebert, *Open J. Phys. Chem.* **2011**, *2*, 123 – 133.
[38] A. Szyk, Z. Wu, K. Tucker, D. Yang, W. Lu, J. Lubkowski, *Protein Sci.* **2006**, *15*, 2749 – 2760.
[39] R. I. Lehrer, G. Jung, P. Ruchala, S. Andre, H. J. Gabius, W. Lu, *J. Immunol.* **2009**, *183*, 480 – 490.
[40] J. M. Schröder, *Immunity* **2014**, *41*, 671 – 673.
[41] J. M. Schröder, *Cell. Mol. Life Sci.* **2006**, *63*, 469 – 486.
[42] R. I. Lehrer, W. Lu, *Immunol. Rev.* **2012**, *245*, 84 – 112.
[43] G. Loers, V. Saini, B. Mishra, F. Papastefanaki, D. Lutz, S. Chaudhury, D. R. Ripoll, A. Wallqvist, S. Gul, M. Schachner, G. Kaur, *J. Neurochem.* **2014**, *128*, 88 – 100.
[44] M. I. Franco, L. Turin, A. Mershin, E. M. C. Skoulakis, *Proc. Natl. Acad. Sci. USA* **2011**, *108*, 3797 – 3802.
[45] A. Seifert, D. Glanz, N. Glaubitz, R. Horstkorte, K. Bork, *Arch. Biochem. Biophys.* **2012**, *524*, 56 – 63.
[46] A. K. Petridis in *Recent Advances in Adhesion Research* (Eds.: A. McFarland, M. Akins), Nova Science, Hauppauge, **2013**, 115 – 122.
[47] A. K. Petridis, A. El Maarouf, U. Rutishauser, *Dev. Dyn.* **2004**, *230*, 675 – 684.
[48] R. Miyahara, F. Tanaka, T. Nakagawa, K. Matsuoka, K. Isii, H. Wada, *J. Surg. Oncol.* **2001**, *77*, 49 – 54.
[49] S. Glüer, C. Schelp, R. Gerardy-Schahn, D. von Schweinitz, *J. Pediatr. Surg.* **1998**, *33*, 1516 – 1520.
[50] S. Glüer, C. Schelp, N. Madry, D. von Schweinitz, M. Eckhardt, R. Gerardy-Schahn, *British J. Cancer* **1998**, *78*, 106 – 110.
[51] M. Suzuki, M. Suzuki, J. Nakayama, A. Suzuki, K. Angata, S. Chen, K. Sakai, K. Hagihara, Y. Yamaguchi, M. Fukuda, *Glycobiology* **2005**, *15*, 887 – 894.
[52] M. C. Amoureux, B. Coulibaly, O. Chinot, A. Loundou, P. Metellus, G. Rougon, D. Figarella-Branger, *BMC Cancer* **2010**, *10*, 91.
[53] H. Cremer, R. Lange, A. Christoph, M. Plomann, G. Vopper, J. Roes, R. Brown, S. Baldwin, P. Kraemer, S. Scheff, *Nature* **1994**, *367*, 455 – 459.
[54] K. Ono, H. Tomasiewicz, T. Magnuson, U. Rutishauser, *Neuron* **1994**, *13*, 595 – 609.
[55] H. Tomasiewicz, K. Ono, D. Yee, C. Thompson, C. Goridis, U. Rutishauser, T. Magnuson, *Neuron* **1993**, *11*, 1163 – 1174.
[56] A. K. Petridis, S. N. Nikolopoulos, A. El-Maarouf, *J. Clin. Neurosci.* **2011**, *18*, 1109 – 1113.
[57] C. S. K. Mayanil, D. George, B. Mania-Farnell, C. L. Bremer, D. McLone, E. G. Bremer, *J. Biol. Chem.* **2000**, *275*, 23259 – 23266.
[58] F. Tanaka, Y. Otake, T. Nakagawa, Y. Kawano, R. Miyahara, M. Li, K. Yanagihara, K. Inui, H. Oyanagi, T. Yamada, J. Nakayama, I. Fujimoto, K. Ikenaka, H. Wada, *Cancer Res.* **2001**, *61*, 1666 – 1670.
[59] J. Roth, C. Zuber, P. Wagner, D. J. Taatjes, C. Weisgerber, P. U. Heitz, C. Goridis, D. Bitter-Suermann, *Proc. Natl. Acad. Sci. USA* **1988**, *85*, 2999 – 3003.
[60] E. Sackmann, F. Keber, D. Heinrich, *Annu. Rev. Condens. Matter Phys.* **2010**, *1*, 257 – 276.
[61] A. El Maarouf, A. K. Petridis, U. Rutishauser, *Proc. Natl. Acad. Sci. USA* **2006**, *103*, 16989 – 16994.
[62] R. Seidenfaden, A. Krauter, F. Schertzinger, R. Gerardy-Schahn, H. Hildebrandt, *Mol. Cell. Biol.* **2003**, *23*, 5908 – 5918.
[63] V. B. Krylov, A. A. Grachev., N. E. Ustyuzhanina, N. A. Ushakova, M. E. Preobrazhenskaya, N. I. Kozlova, M. N. Portsel, I. N. Konovalova, V. Y. Novikov, H.-C. Siebert, A. S. Shashkov, N. E. Nifantiev, *Russian Chem. Bull. (Med. Chem. Issue) Int. Ed.* **2011**, *60*, 746 – 753.
[64] H.-C. Siebert, M. Burg-Roderfeld, T. Eckert, S. Stötzel, U. Kirch, T. Diercks, M. J. Humphries, M. Frank, R. Wechselberger, E. Tajkhorshid, S. Oesser, *Protein Cell* **2010**, *1*, 393 – 405.
[65] O. Raabe, C. Reich, S. Wenisch, A. Hild, M. Burg-Roderfeld, H.-C. Siebert, S. Arnhold, *Histochem. Cell Biol.* **2010**, *134*, 545 – 554.
[66] S. Schadow, H.-C. Siebert, G. Lochnit, J. Kordelle, M. Rickert, J. Steinmeyer, *PLoS One* **2013**, *8*, e53955.
[67] A. Mehanna, I. Jakovcevski, A. Acar, M. Xiao, G. Loers, G. Rougon, A. Irintchev, M. Schachner, *Mol. Ther.* **2010**, *18*, 34 – 43.
[68] P. Marino, J. C. Norreel, M. Schachner, G. Rougon, M. C. Amoureux, *Exp. Neurol.* **2009**, *219*, 163 – 174.
[69] S. G. Cajal, *Histology of the Nervous System of Man and Vertebrates*, Vol. 1 and 2, Oxford University Press, London, **1928**.
[70] G. Loers, T. Makhina, U. Bork, A. Dörner, M. Schachner, R. Kleene, *J. Neurosci.* **2012**, *32*, 3917 – 3930.
[71] M. Sumida, M. Hane, U. Yabe, Y. Shimoda, O. M. T. Pearce, M. Kiso, T. Miyagi, M. Sawada, A. Varki, K. Kitajima, C. Sato, *J. Biol. Chem.* **2015**, *290*, 13202 – 13214..
[72] H.-C. Siebert, R. Zhang, A. Scheidig, T. Eckert, H. Wienk, R. Boelens, M. Mahvash, A. K. Petridis, R. Schauer, *J. Neurol. Disord.* **2015**, *3*, 212.
[73] J. Harder, J. M. Schröder, *J. Leukocyte Biol.* **2005**, *77*, 476 – 486.

[74] J. Jeener, B. H. Meier, P. Bachmann, R. R. Ernst, *J. Chem. Phys.* **1979**, *71*, 4546 – 4553.
[75] L. Braunschweiler, R. R. Ernst, *J. Magn. Reson.* **1983**, *53*, 521 – 528.
[76] A. Bernardi, D. Potenza, A. M. Capelli, A. García-Herrero, F. J. Canada, J. Jiménez-Barbero, *Chem. Eur. J.* **2002**, *8*, 4598 – 4612.
[77] W. L. De Lano, De Lano Scientific, San Carlos, CA (USA), **2002**.
[78] G. Loers, S. Chen, M. Grumet, M. Schachner, *J. Neurochem.* **2005**, *92*, 1463 – 1476.
[79] I. Jakovcevski, J. Siering, G. Hargus, N. Karl, L. Hoelters, N. Djogo, S. Yin, N. Zecevic, M. Schachner, A. Irintchev, *J. Comp. Neurol.* **2009**, *513*, 496 – 510.
[80] I. Kalus, B. Schnegelsberg, N. G. Seidah, R. Kleene, M. Schachner, *J. Biol. Chem.* **2003**, *278*, 10381 – 10388.
[81] S. Lü, S. Liang, X. Gu, *J. Protein Chem.* **1999**, *18*, 609 – 617.
[82] J. Schindelin, I. Arganda-Carreras, E. Frise, V. Kaynig, M. Longair, T. Pietzsch, S. Preibisch, C. Rueden, S. Saalfeld, B. Schmid, J. Y. Tinevez, D. J. White, V. Hartenstein, K. Eliceiri, P. Tomancak, A. Cardona, *Nat. Methods* **2012**, *9*, 676 – 682.

Received: December 30, 2015
Revised: March 1, 2016
Published online on ■■ ■■, 0000

*R. Zhang, G. Loers, M. Schachner, R. Boelens, H. Wienk, S. Siebert, T. Eckert, S. Kraan, M. A. Rojas-Macias, T. Lütteke, S. P. Galuska, A. Scheidig, A. K. Petridis, S. Liang, M. Billeter, R. Schauer, J. Steinmeyer, J.-M. Schröder, H.-C. Siebert**

■■ – ■■

Molecular Basis of the Receptor Interactions of Polysialic Acid (polySia), polySia Mimetics, and Sulfated Polysaccharides

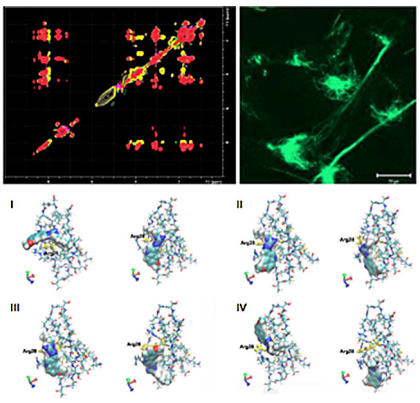

Submolecular polySia interactions: Specific interactions of polysialic acid (polySia) and polySia glycomimetic molecules were studied at the submolecular level using a combination of NMR and molecular modeling. The structure–function interplay between polySia or sulfated polysaccharides and their receptors can be exploited to develop new drugs and application routes for the treatment of neurological diseases and dysfunctions.

Submolecular polysialic acid studies: #DrugDevelopment for #NeurologicalDisease @KielUni SPACE RESERVED FOR IMAGE AND LINK

Share your work on social media! *ChemMedChem* has added Twitter as a means to promote your article. Twitter is an online microblogging service that enables its users to send and read text-based messages of up to 140 characters, known as "tweets". Please check the pre-written tweet in the galley proofs for accuracy. Should you or your institute have a Twitter account, please let us know the appropriate username (i.e., @accountname), and we will do our best to include this information in the tweet. This tweet will be posted to the journal's Twitter account @ChemMedChem (follow us!) upon online publication of your article, and we recommended you to repost ("retweet") it to alert other researchers about your publication.

Please check that the ORCID identifiers listed below are correct. We encourage all authors to provide an ORCID identifier for each coauthor. ORCID is a registry that provides researchers with a unique digital identifier. Some funding agencies recommend or even require the inclusion of ORCID IDs in all published articles, and authors should consult their funding agency guidelines for details. Registration is easy and free; for further information, see http://orcid.org/.

Ruiyan Zhang
Dr. Gabriele Loers
Prof. Dr. Melitta Schachner
Prof. Dr. Rolf Boelens
Dr. Hans Wienk
Simone Siebert
Dr. Thomas Eckert
Dr. Stefan Kraan
Miguel A. Rojas-Macias
Dr. Thomas Lütteke http://orcid.org/0000-0002-7140-9933
Dr. Sebastian P. Galuska
Prof. Dr. Axel Scheidig
Dr. Athanasios K. Petridis
Prof. Dr. Songping Liang
Prof. Dr. Martin Billeter
Prof. Dr. Roland Schauer
Prof. Dr. Jürgen Steinmeyer
Prof. Dr. Jens-Michael Schröder
Prof. Dr. Hans-Christian Siebert